

NEW RESEARCH IN

Physical Sciences 

Social Sciences 

Biological Sciences 

Air-quality implications of widespread adoption of cool roofs on ozone and particulate matter in southern California



Scott A. Epstein, Sang-Mi Lee, Aaron S. Katzenstein, Marc Carreras-Sospedra, Xinqiu Zhang, Salvatore C. Farina, Pouya Vahmani, Philip M. Fine, and George Ban-Weiss

PNAS August 7, 2017. 201703560; published ahead of print August 7, 2017. <https://doi.org/10.1073/pnas.1703560114>

Edited by Christopher B. Field, Stanford University, Stanford, CA, and approved July 5, 2017 (received for review March 8, 2017)

Article

Figures & SI

Authors & Info

 PDF

Significance

The South Coast Air Basin of California, a region of 16.8 million people, is among the most polluted air basins in the United States. A multidecadal effort to attain federal air-quality standards has led to significant progress, but much more work remains. Are recently implemented statewide building efficiency standards on rooftops counterproductive to these goals? With comprehensive regional models and intensive development of model input parameters, our research has identified the air-quality consequences that are expected to result from these efficiency standards. The results can

We use cookies on this site to enhance your user experience. By clicking any link on this page you are giving your consent for us to set cookies.

Continue

Find out more

inform policies to mitigate some air-quality penalties, while preserving the benefits of building efficiency standards. This work also sheds light on potential future policies aimed at reducing urban heating from pavement surfaces.

Abstract

The installation of roofing materials with increased solar reflectance (i.e., “cool roofs”) can mitigate the urban heat island effect and reduce energy use. In addition, meteorological changes, along with the possibility of enhanced UV reflection from these surfaces, can have complex impacts on ozone and PM_{2.5} concentrations. We aim to evaluate the air-quality impacts of widespread cool-roof installations prescribed by California’s Title 24 building energy efficiency standards within the heavily populated and polluted South Coast Air Basin (SoCAB). Development of a comprehensive rooftop area database and evaluation of spectral reflectance measurements of roofing materials allows us to project potential future changes in solar and UV reflectance for simulations using the Weather Research Forecast and Community Multiscale Air Quality (CMAQ) models. 2012 meteorological simulations indicate a decrease in daily maximum temperatures, daily maximum boundary layer heights, and ventilation coefficients throughout the SoCAB upon widespread installation of cool roofs. CMAQ simulations show significant increases in PM_{2.5} concentrations and policy-relevant design values. Changes in 8-h ozone concentrations depend on the potential change in UV reflectance, ranging from a decrease in population-weighted concentrations when UV reflectance remains unchanged to an increase when changes in UV reflectance are at an upper bound. However, 8-h policy-relevant ozone design values increase in all cases. Although the other benefits of cool roofs could outweigh small air-quality penalties, UV reflectance standards for cool roofing materials could mitigate these negative consequences. Results of this study motivate the careful consideration of future rooftop and pavement solar reflectance modification policies.

urban air quality albedo California Title 24 Los Angeles urban surface modification

The South Coast Air Basin (SoCAB) is a region of southern California encompassing Orange County and the urban portions of Los Angeles, San Bernardino, and Riverside counties. With 16.8 million people, the SoCAB is the second most populous urban area in the United States. A fossil-fuel-dependent transit and goods movement infrastructure along with a well-developed industrial presence within the 27,824-km² SoCAB generates significant emissions of oxides of nitrogen (NO_x), volatile organic compounds (VOCs), directly emitted primary particulate matter (PM), and secondary PM precursors. Persistent high-pressure systems, ample photochemistry, infrequent rainfall, and ventilation-inhibiting topography also contribute to severe air-quality problems. The SoCAB currently does not attain federal air-quality standards for 8-h O₃, 1-h O₃, annual-averaged PM_{2.5}, and 24-h PM_{2.5}. Ozone levels within the SoCAB are often the highest in the nation (1).

By clicking any link on this page you are giving your consent for us to set cookies.

[Continue](#)

[Find out more](#)

The hot and sunny conditions typically experienced within the SoCAB make urban surface modification a useful strategy to reduce urban temperatures. Meteorological impacts of roofing materials with enhanced solar reflectance (SR, synonymous with “albedo”), colloquially referred to as “cool roofs,” are well-studied and indicate several benefits in urban areas. The replacement of darker materials with high-reflectance surfaces within cities can help mitigate the urban heat island effect

(2–14). Moreover, meteorological modeling suggests that the deployment of cool roofs will reduce afternoon summertime temperatures, leading to reduced cooling energy demands, resulting in a curtailment of greenhouse gas emissions (15, 16) in most urban areas. Cool roofs will also lower the Earth’s radiative forcing by increasing the global albedo (17–19), although impacts on global climate remain unsettled in the literature (20), with recent research suggesting effects are negligible (4).

Cool roofs can affect air quality through several mechanisms, although there are far fewer studies investigating these effects compared with the wealth of meteorological and climatological studies. Because the air-quality effects of urban surface modification by cool roofs are complex and nonlinear, comprehensive emissions processing, meteorological, and chemical transport models are needed to accurately determine potential impacts on air quality for policy-making purposes. Potential changes in mixing height and ventilation (21) will affect ambient pollutant concentrations. Cool roofs can reduce temperature-dependent emissions of precursors to O₃ and PM in urban areas by lowering ambient temperatures, resulting in a slower rate of VOC evaporation and NO_x emissions (14). In addition, the atmospheric reactions that produce O₃ are slower at lower temperatures. A handful of studies modeled the effect of cool-roof installations on O₃ concentrations during short-term multiday O₃ episodes in the SoCAB (22–26). Population-weighted O₃ exposures were reduced with an increase in urban SR; however, O₃ concentrations in the less-populated eastern SoCAB exhibited O₃ increases. Further increases in surface SR led to smaller net reductions in O₃ because significant weakening of the sea breeze led to reduced vertical mixing.

To the authors’ knowledge, all but one (29) of the previous studies investigating the role of cool-roof materials on air quality assume that widespread adoption of cool roofs will not change UV reflectance (UVR) (2, 22–27). Increases in UVR can significantly affect photochemical production of O₃. For example, O₃ concentrations in the Uintah Basin are elevated in the winter during periods of snow cover due to increased UV reflectivity and limited mixing from reduced surface heating (28). Fallmann et al. (29) modified building SR for all urban grid cells in Stuttgart, Germany from 0.2 to 0.7 across all wavelengths. Although this increase in UVR is unrealistically high, the authors saw a significant increase in peak O₃ concentrations during a clear-sky, sunny period, which they attribute to increases in reflected UV radiation.

In this research effort we aim to rigorously evaluate the air-quality effects in the SoCAB of current cool-roof installation policies in California Title 24 Building Energy Efficiency Standards (Title24) (30). Besides O₃, we also focus on PM_{2.5} concentrations, a pollutant that largely drives the health impacts of air

newly analyzed data on the UVR of hundreds of real-world roofing products, we directly evaluate the assumption used in previous studies that standard and cool roofs have nearly the same UVR and then probe the sensitivity of UVR on resulting pollutant concentrations. Rather than focusing on specific air-pollution episodes, we have conducted a collection of comprehensive simulations over an entire calendar year. We developed a high-resolution database of building rooftop areas classified by land-use category to project future SR after full implementation of Title24 standards in the SoCAB. WRF v3.6, a state-of-the-science meteorological model, was used to forecast changes in meteorology induced by cool roofs. The temperature-dependent 2012 SoCAB emissions inventory (1) and a modified version of the state-of-the-science Community Multiscale Air Quality Model (CMAQ version 5.0.2) were then used to project future O₃ and PM_{2.5} concentrations after cool-roof implementation.

Materials and Methods

Projecting Future SR.

Determining the effects of Title24 standards on SR requires information on the current SR and the total rooftop area in each Title24 building category. Title24 standards prescribe that new or renovated rooftops meet SR standards that are based on climate zone (SI Appendix, Fig. S1) and building type (30) (Table 1). We determined the rooftop area of each Title24 building category in every model grid cell with land-use data for 2012 from the Southern California Association of Governments (SCAG) and building footprint data from the US Army Corps of Engineers (32). See SI Appendix.

Table 1.

[VIEW INLINE](#) [VIEW POPUP](#)

Current and future SR values corresponding to Title24 categories

We used monthly Moderate Resolution Imaging Spectroradiometer (MODIS) measurements of SR (33) to determine base-case values for each 4-km model grid cell. The current SR of rooftops for each Title24 category in the SoCAB was calculated by combining recent aircraft-based remote sensing measurements of rooftops in Los Angeles and Long Beach, CA (8, 9) with SCAG land-use data (Table 1). The projected future building SR, set by the Title24 standards, along with the current building SR, calculated with the remote sensing measurement data, allowed us to determine the expected change in SR in the fraction of each grid cell occupied by buildings and determine the monthly SR for each grid cell if all rooftops meet Title24 standards. Fig. 1A details the calculated change in grid-cell average SR in response to full implementation of Title24 standards.

We use cookies on this site to enhance your user experience. By clicking any link on this page you are giving your consent for us to set cookies.

[Continue](#)

[Find out more](#)



[Download figure](#)

[Open in new tab](#)

[Download powerpoint](#)

Fig. 1.

(A) Change in SR (Title24 – baseline) used for WRF simulations. (B) Maximum possible change in UVR (Title24 – baseline) used for CMAQ simulations.

Projecting UVR for Chemical Transport Modeling.

Photolysis reactions are wavelength-dependent (34); therefore, capturing changes in photochemistry from Title24 requires careful consideration of wavelength-dependent reflectances. In situ remote sensing measurements of rooftop UVR are not available. However, several studies measured the wavelength-dependent spectral reflectance of roofing materials (8, 9, 35–37). To bound the possible change in wavelength-dependent reflectance, Fig. 2 presents spectral reflectance measurements (8, 9) for a wide variety of traditional and cool roof materials as a function of wavelength for high slope (Fig. 2A) and low slope (Fig. 2B) roofing materials (SI Appendix, Table S2). We define cool roofs, based on Title24 standards, as those with an SR above 0.20 and 0.63 for low-slope and high-slope roofing materials, respectively. To serve as an extreme upper-bound increase in UVR, we set the maximum change in reflectance at each CMAQ wavelength range to be the largest difference between the cool and standard roofing materials (Fig. 1B) and applied these differences based on their corresponding area in each grid cell. Projection

We use cookies on this site to enhance your user experience. By clicking any link on this page you are giving your consent for us to set cookies.

[Continue](#)

[Find out more](#)

categories

comprehensively in the SI Appendix. We also explored the scenario where UVR does not change to serve as a lower bound. Each of these scenarios was used to drive photochemistry in the Title24 simulations in CMAQ. The Title24 SR changes as derived in the previous paragraph were used for the 410- to 850-nm wavelength band in the CMAQ simulations.



[Download figure](#)

[Open in new tab](#)

[Download powerpoint](#)

Fig. 2.

Range of wavelength-dependent reflectance of cool and standard roofing materials for high-slope (A) and low-slope (B) applications.

Emissions Processing.

On-road NO_x and VOC along with biogenic VOC emissions profiles are dependent on meteorology. Annual hourly emissions profiles were developed as a function of the baseline and Title24 meteorological fields for the 2012 base year. The SoCAB emissions inventory is presented in ref. **1** and details of the emissions processing are presented in ref. **38**. Changes in NO_x and VOC emissions in the baseline and Title24 simulations are small, mainly due to the similarity in the meteorological fields.

Within the SoCAB, on average during the O₃ season, VOC emissions are reduced by 8 × 10⁻⁴% (0.004%) and NO_x emissions are reduced by 8 × 10⁻⁴% (0.004%) per day).

We use cookies on this site to enhance your user experience. By clicking any link on this page you are giving your consent to our use of cookies.

[Continue](#)

[Find out more](#)

Within the SoCAB, changes in power-generation emissions are expected to be insignificant with the widespread implementation of cool roofs and are not accounted for in the modeling. Emissions from power generation are only responsible for 0.4% of the total NO_x emissions in the 2012 emission inventory. Additionally, only 37% of the total electricity consumed is generated within the SoCAB (1).

Meteorological and Chemical Transport Modeling.

WRF version 3.6.1 was used with a North American Regional Reanalysis field to simulate 2012 meteorology on three nested grids, with an inner 4-km grid covering the modeling domain (SI Appendix, Fig. S9). (Details of the model setup are available in ref. 38.) WRF model performance is summarized in SI Appendix, Figs. S10–S19. Two year-long simulations were performed: a base case using the MODIS-derived SR fields and a Title24 case using the modified SR fields detailed above assuming that all buildings in the SoCAB meet Title24 rooftop SR requirements.

CMAQ version 5.0.2 was used to simulate air quality without dynamic coupling within a 624- × 408-km modeling domain on a 4-km grid with 18 vertical layers. Extensive details of the modeling protocol are presented in ref. 38. Modification of the CMAQ code allowed us to calculate spatially resolved photolysis rate constants based on wavelength-dependent reflectance fields. As with any modeling study, results are dependent on the model accurately capturing the physical and chemical processes under investigation. SI Appendix, Figs. S20–S28 summarize the ability of CMAQ to predict measured concentrations of O₃ and PM_{2.5} throughout the SoCAB.

Changes in annual averaged PM_{2.5}, daily maximum 8-h O₃, and daily maximum 1-h O₃ concentrations were evaluated across the modeling domain. Student's t tests for paired samples were conducted to determine whether changes in concentration across different scenarios were statistically significant. Differences with P values less than 0.05 were assumed to be statistically significant.

To evaluate the impact of widespread cool-roof installation toward attainment of federal ambient air-quality standards, relative response factor projections were also conducted to calculate changes in design values (DV). This strategy uses the ratio of Title24 vs. baseline concentrations to adjust measured values, cancelling out many of the systematic uncertainties responsible for concentration biases. This analysis is consistent with Environmental Protection Agency (EPA) modeling guidance (39) and is presented in ref. 38 with a summary in SI Appendix. Data and scripts, with minor exclusions (SI Appendix), are available with a South Coast Air Quality Management District public records request.

Results and Discussion

Changes in Meteorology.

WRF simulations of 2012 meteorology representing the baseline (MODIS-derived SR) and Title24 (SR modified for cool-roof adoption) cases are summarized in Fig. 1. WRF model temperatures are projected to decrease throughout the SoCAB.

We use cookies on this site to enhance your user experience. By clicking any link on this page you are giving your consent for us to set cookies.

[Continue](#)

[Find out more](#)

(-0.35 K) in areas with the largest change in SR. Changes in the daily maximum planetary boundary layer height (PBLH) (**Fig. 3B**) are negative; the mixed layer height will decrease by 40–65 m in the most polluted areas of the SoCAB in the Title24 scenario, a significant difference compared with model-predicted average daily maximum mixed layer heights of 1–2 km. A decrease in surface temperature can reduce the buoyancy of the surface air, leading to a reduction in vertical mixing. Lower surface temperatures on land decrease the land–sea temperature gradient, slowing down the daytime sea breeze—an important mechanism that drives relatively clean marine air into the SoCAB. The average of the 9 AM-to-3 AM ventilation coefficient (VC), the integral of the horizontal wind velocity with respect to height at all layers below the maximum mixing depth (**40**) (**Fig. 3C**), decreases throughout the SoCAB with implementation of Title24. Daily profiles of the change in several meteorological variables are presented in SI Appendix, Figs. S29–S32.



[Download figure](#)

[Open in new tab](#)

[Download powerpoint](#)

Fig. 3. (A) Change in annual average daily max temperatures (Title24 – baseline). (B) Change in annual average daily maximum PBLH. (C) Change in annual average VC calculated between 9 AM and 3 PM. Gray hashed cells indicate that differences are not statistically significant ($P > 0.05$).

We use cookies on this site to enhance your user experience. By clicking any link on this page you are giving your consent for us to set cookies.

[Continue](#)

[Find out more](#)

Changes in PM_{2.5} Concentrations.

Several year-long CMAQ simulations were conducted to determine the individual effects of changes in meteorology, emissions, enhanced SR, and a range of hypothetical changes in UVR. **Fig. 4A** shows the change in annual PM_{2.5} concentrations between the baseline simulation (scenario I in **Table 2**) and a simulation using Title24 meteorology, emissions resulting from the Title24 meteorology, and the assumption that UVR does not increase (scenario IV). Average PM_{2.5} concentrations increase throughout the SoCAB, presumably caused by reductions in mixing heights and VCs, as well as partitioning of semivolatile species to the particle phase at lower temperatures. In the populated central Los Angeles region and Long Beach, annual PM_{2.5} concentrations are projected to increase by approximately $0.3 \mu\text{g} \cdot \text{m}^{-3}$. **Fig. 4B** illustrates the change in the number of days that exceed the 24-h PM_{2.5} standard of $35 \mu\text{g} \cdot \text{m}^{-3}$ (scenario IV – scenario I). These changes are location-dependent, with increases in Los Angeles and the Inland Empire where PM_{2.5} is typically highest.



[Download figure](#)

[Open in new tab](#)

[Download powerpoint](#)

Fig. 4.

(A) Change in annual average PM_{2.5} concentrations (scenario IV – scenario I). The green circle indicates the location of the highest annual PM_{2.5} measured DVs in the basin. Seasonal differences in PM_{2.5} concentrations are shown in CMAQ simulations. (B) Change in the number of 24-h PM_{2.5} federal standard ($35 \mu\text{g} \cdot \text{m}^{-3}$) exceedance days. Hashed cells indicate that differences are not statistically significant ($P > 0.05$).

[Continue](#)

[Find out more](#)

Gray
age.

Table 2.[VIEW INLINE](#) [VIEW POPUP](#)Simulated changes in PM_{2.5} and O₃ at polluted locations

Changes in annual averaged PM_{2.5} at the Mira Loma monitoring location—the most polluted PM_{2.5} station in the SoCAB—for each simulation are presented in **Table 2**. Implementation of Title24 emissions (scenario III) does not affect PM_{2.5} concentrations relative to the baseline scenario (scenario I). However, the inclusion of Title24 meteorology (scenario IV) leads to an annual average PM_{2.5} increase of $0.19 \pm 0.007 \mu\text{g} \cdot \text{m}^{-3}$. Increases in UVR (scenario V) lead to minimal changes in PM_{2.5} concentrations.

Changes in SoCAB maximum annual and 24-h PM_{2.5} policy-relevant DVs calculated with the EPA-recommended relative response factor approach are also shown in **Table 2**. SoCAB maximum annual DVs are expected to increase by approximately $0.2 \mu\text{g} \cdot \text{m}^{-3}$ even if increases in UVR are avoided—important compared with the $12 \mu\text{g} \cdot \text{m}^{-3}$ federal standards. Twenty-four-hour PM_{2.5} DVs are projected to increase by $0.62\text{--}0.65 \mu\text{g} \cdot \text{m}^{-3}$ depending on changes in UVR—important compared with the 24-h PM_{2.5} standard of $35 \mu\text{g} \cdot \text{m}^{-3}$.

Changes in Ozone Concentrations.

Fig. 5 shows changes in daily maximum 8-h O₃ (DM8HO₃) concentrations averaged over the O₃ season (May 1–September 30) for two scenarios. **Fig. 5A** shows the changes expected if Title24 were fully implemented but UVR was held constant (scenario IV – scenario I). O₃ concentrations largely decrease throughout the SoCAB, with the exception of the Redlands area, which typically experiences the highest O₃ concentrations in the SoCAB. However, most residents in the SoCAB live in areas that will experience a decrease in O₃ under this scenario. Whereas the number of 75 ppb exceedance days is relatively unchanged in the most populated areas of the SoCAB, the number of exceedance days increase in the region surrounding Redlands (SI Appendix, Fig. S35A). **Fig. 5B** shows changes in O₃ concentrations resulting from an upper-bound change in UVR (scenario V – scenario I). Increases in average DM8HO₃ concentrations are expected in most of the SoCAB in this scenario (**Fig. 5B**). This translates to large increases in the number of exceedance days throughout the SoCAB (SI Appendix, Fig. S35A).

We use cookies on this site to enhance your user experience. By clicking any link on this page you are giving your consent for us to set cookies.

[Continue](#)[Find out more](#)



[Download figure](#)

[Open in new tab](#)

[Download powerpoint](#)

Fig. 5.

(A) Change in annual average DM8HO₃ values (scenario IV) with the assumption that UVR does not change with widespread installation of cool roofs. The green circle indicates the location of the highest 8-h O₃ measured DVs in the basin. (B) Change in annual average DM8HO₃ values with the assumption that UVR increases are consistent with the maximum possible increase based on roofing products currently available (scenario V). Gray hashed cells indicate that differences are not statistically significant ($P > 0.05$). Image represents 3- × 3-cell moving average.

Table 2 details changes in mean +/- standard error (SE) DM8HO₃ concentrations at Redlands, the station with the highest 8-h O₃ DV. Changes in 1-h averaged daily maximum O₃ (DM1HO₃) concentrations are presented for Fontana, the monitoring station with the highest 1-h DVs in the SoCAB. Ozone concentrations are neither sensitive to increases in visible and IR reflectance (scenario II) within CMAQ nor to decreases in emissions inherent in the Title24 scenario (scenario III). Simulations with Title24 meteorology produce increases in averaged DM8HO₃ concentrations (scenarios IV and V). Depending on the magnitude of UVR increases, DM8HO₃ concentrations are projected to increase by 0.04 ± 0.013 (scenario IV) to 0.66 ± 0.015 ppb (scenario V), whereas DM1HO₃ concentrations are projected to change by -0.040 ± 0.023 to 0.96 ± 0.026 ppb. Although the increase in UVR in the upper-bound case is relatively small, ranging from 0 to 0.027 depending on the scenario, ozone formation is still extremely sensitive to these increases. The projected change in ozone for 8-h

We use cookies on this site to enhance your user experience. By clicking any link on this page you are giving your consent to our use of cookies.

[Continue](#)

[Find out more](#)

and 1-h O₃ are presented in **Table 2**. Changes in O₃ concentrations and DVs are linearly dependent on the degree of UVR increases (SI Appendix, Fig. S33 and Table S1). The SoCAB maximum 8-h DV increases by 0.3 ppb with a constant UVR across the domain to 1.3 ppb with the UVR at the upper bound. Behavior of the 1-h SoCAB maximum DV is more complex. If increases in UVR can be avoided, the 1-h DV is expected to decrease by 0.4 ppb. However, if concentrations are simulated with maximum increases in UVR, 1-h O₃ DV concentrations can increase by 1.9 ppb. This counterintuitive behavior can be explained partially with **Fig. 5**. Fontana is further west than Redlands and is in the region where O₃ concentrations decrease when UVR is held constant and increase when UVR is at its maximum value. This illustrates the competition between the many factors governing O₃ concentrations that can change with cool-roof implementation.

Policy Implications.

Attainment of the 75-ppb 8-h O₃ standard by 2031 in the SoCAB is an extremely challenging air-quality goal, requiring an additional 55% reduction in NOx emissions beyond all existing regulations (1). Compliance with Title24 cool-roof standards may make attainment of this goal more difficult, even if future UVR increases are small. Scenario V assumes that buildings adopt cool roofing products with increase in UVR at an extreme upper bound. The actual increases in UVR throughout the SoCAB will depend on the individual roofing products that are chosen for installation. Although more realistic UVR increases cannot be projected without knowledge of the individual cool roofing products that are adopted, our analysis indicates that UVR will likely increase when replacing standard roofs with cool roofs. Whether ozone ultimately increases or decreases in the most populated areas of the basin will depend on the relative importance of multiple physicochemical pathways, including ozone decreases from temperature reductions, ozone increases from reduced ventilation and mixing, and ozone increases from possible UVR increases. Different magnitudes of SR increase or UVR increase may change the dominating mechanisms. We also simulated 2031 DVs with the presence of full Title24 implementation and full implementation of the proposed South Coast Air Quality Management District control strategy (1). We estimate that even if UVR increases can be entirely avoided, Title24 could increase the 2031 8-h DV by 0.3 ppb and the 2031 1-h DV by 1.1 ppb. These increases in O₃ concentrations are consequential in light of the cost to reduce precursor emissions to achieve a corresponding reduction in O₃ concentrations.

Implementation of Title24 standards was used as the basis for this analysis; however, several factors may influence future adoption of cool roofs. Municipalities such as Los Angeles and Pasadena have cool-roof ordinances that can lead to increases in SR beyond what would be expected with the Title24 standards. In addition, widespread adoption of solar photovoltaics and Title24 cool-roof installation exemptions for the implementation of equivalent energy savings measures could also affect future changes in urban reflectance.

The O₃ concentration sensitivity to small changes in cool-roof UVR supports the establishment of a standard regulating the UVR of certified cool-roof materials. Cool-roof materials that are certified for us to set cookies. Establish standards for consideration as a cool-roof material. Establish

We use cookies on this site to enhance your user experience. By regulating the UVR of certified cool-roof materials. Cool-roof materials that are certified for us to set cookies.

Continue

Find out more

ific SR could

help minimize inadvertent increases in O_3 . Furthermore, it is possible that a reduction in UVR below current values will lead to improvements in O_3 air quality throughout the SoCAB; this may be a cost-effective O_3 control strategy. Remote sensing measurements of the current rooftop stock to survey UVR could help set standards such that cool-roof materials do not lead to increases in UVR when they replace existing rooftops.

When assessing the impacts of cool roofs, it is important to consider all environmental and economic consequences. For example, benefits from a reduction in heat-related mortality may outweigh the increase in mortality from enhanced $PM_{2.5}$ pollution. Also, widespread increases in urban SR can help to combat the local impacts of climate change. Potential energy bill savings are also an important benefit. In addition, there are other mechanisms to control ambient air pollution such as emission reductions, whereas tools for mitigation of the urban heat island effect are more limited. Without a comprehensive analysis of all of the benefits of cool roofs it would be a mistake to discourage this technology solely on the basis of air quality alone.

Relatively small changes in surface reflectance lead to significant impacts in O_3 and $PM_{2.5}$. Results of this analysis also shed light on the choice of pavement materials and cool pavements, a potentially more important driver of overall urban SR and UVR. Analysis of impervious surface area (41) along with the rooftop area database developed for this paper indicates that there is significantly more pavement area in the SoCAB than rooftop area (1,900 km^2 of pavement area vs. 1,040 km^2 of rooftop area). (SI Appendix, Fig. S36 presents the spatial distribution of pavement area throughout the SoCAB.) In addition, only a fraction of the total rooftop area was modified for projections of air quality because Title24 does not affect rooftops in every climate zone. Therefore, the SR and UVR of pavements may be an important driver of regional air quality and human exposure to UV radiation and should be considered when evaluating cool pavement materials.

Acknowledgments

This work was funded in part by NSF Grant CBET-1512429 (to G.B.-W.).

Footnotes

↩¹To whom correspondence should be addressed. Email: sepstein@aqmd.gov.

Author contributions: S.A.E., S.-M.L., A.S.K., P.M.F., and G.B.-W. designed research; S.A.E., M.C.-S., X.Z., S.C.F., P.V., and G.B.-W. performed research; S.A.E. and S.C.F. contributed new reagents/analytic tools; S.A.E. and G.B.-W. analyzed data; and S.A.E. and G.B.-W. wrote the paper.

We use cookies on this site to enhance your user experience. By clicking any link on this page you are giving your consent for us to set cookies.

Continue

Find out more

The authors declare no conflict of interest.

This article is a PNAS Direct Submission.

This article contains supporting information online at
www.pnas.org/lookup/suppl/doi:10.1073/pnas.1703560114/-/DCSupplemental.

References

1. ↪South Coast Air Quality Management District (2016) Final 2016 air quality management plan (South Coast Air Quality Management District, Diamond Bar, CA). . [Google Scholar](#)
2. ↪Akbari H, Pomerantz M, Taha H (2001) Cool surfaces and shade trees to reduce energy use and improve air quality in urban areas. *Sol Energy* **70**:295–310. . [CrossRef](#) [Google Scholar](#)
3. ↪Vahmani P, Sun F, Hall A, Ban-Weiss G (2016) Investigating the climate impacts of urbanization and the potential for cool roofs to counter future climate change in Southern California. *Environ Res Lett* **11**:124027. . [Google Scholar](#)
4. ↪Zhang J, Zhang K, Liu J, Ban-Weiss G (2016) Revisiting the climate impacts of cool roofs around the globe using an Earth system model. *Environ Res Lett* **11**:084014. . [Google Scholar](#)
5. ↪Stone B Jr, et al. (2014) Avoided heat-related mortality through climate adaptation strategies in three US cities. *PLoS One* **9**:e100852. . [CrossRef](#) [PubMed](#) [Google Scholar](#)
6. ↪Georgescu M, Morefield PE, Bierwagen BG, Weaver CP (2014) Urban adaptation can roll back warming of emerging megapolitan regions. *Proc Natl Acad Sci USA* **111**:2909–2914. . [Abstract/FREE Full Text](#) [Google Scholar](#)
7. ↪Santamouris M (2014) Cooling the cities: A review of reflective and green roof mitigation technologies to fight heat island and improve comfort in urban environments. *Sol Energy* **103**:682–703. . [CrossRef](#) [Google Scholar](#)
8. ↪Ban-Weiss GA, Woods J, Levinson R (2015) Using remote sensing to quantify albedo of roofs in seven California cities, part 1: Methods. *Sol Energy* **115**:777–790. . [Google Scholar](#)
9. ↪Ban-Weiss GA, Woods J, Millstein D, Levinson R (2015) Using remote sensing to quantify albedo of roofs in seven California cities, part 2: Results and application to climate modeling. *Sol Energy* **115**:791–805. . [Google Scholar](#)
10. ↪Li D, Bou-Zeid E, Oppenheimer M (2014) The effectiveness of cool and green roofs as urban heat island mitigation strategies. *Environ Res Lett* **9**:055002. . [Google Scholar](#)
11. ↪Doulos L, Santamouris M, Livada I (2004) Passive cooling of outdoor urban spaces: The role of materials. *Sol Energy* **77**:231–249. . [Google Scholar](#)

By clicking any link on this page you are giving your consent for us to set cookies.

[Continue](#)

[Find out more](#)

12. ←Santamouris M, Synnefa A, Karlessi T (2011) Using advanced cool materials in the urban built environment to mitigate heat islands and improve thermal comfort conditions. *Sol Energy* **85**:3085–3102. . [CrossRef](#)
[Google Scholar](#)
13. ←Li D, Bou-Zeid E (2013) Synergistic interactions between urban heat islands and heat waves: The impact in cities is larger than the sum of its parts. *J Appl Meteorol Climatol* **52**:2051–2064. . [Google Scholar](#)
14. ←Millstein D, Menon S (2011) Regional climate consequences of large-scale cool roof and photovoltaic array deployment. *Environ Res Lett* **6**:034001. . [Google Scholar](#)
15. ←Akbari H, Levinson R (2008) Evolution of cool-roof standards in the US. *Adv Build Energy Res* **2**:1–32. .
[Google Scholar](#)
16. ←Levinson R, Akbari H (2009) Potential benefits of cool roofs on commercial buildings: Conserving energy, saving money, and reducing emission of greenhouse gases and air pollutants. *Energy Effic* **3**:53–109. .
[Google Scholar](#)
17. ←Menon S, Akbari H, Mahanama S, Sednev I, Levinson R (2010) Radiative forcing and temperature response to changes in urban albedos and associated CO₂ offsets. *Environ Res Lett* **5**:014005. . [Google Scholar](#)
18. ←Akbari H, Menon S, Rosenfeld A (2009) Global cooling: Increasing world-wide urban albedos to offset CO₂. *Clim Change* **94**:275–286. . [Google Scholar](#)
19. ←Akbari H, Matthews HD, Seto D (2012) The long-term effect of increasing the albedo of urban areas. *Environ Res Lett* **7**:024004. . [Google Scholar](#)
20. ←Jacobson MZ, Ten Hoeve JE (2011) Effects of urban surfaces and white roofs on global and regional climate. *J Clim* **25**:1028–1044. . [Google Scholar](#)
21. ←Sharma A, et al. (2016) Green and cool roofs to mitigate urban heat island effects in the Chicago metropolitan area: Evaluation with a regional climate model. *Environ Res Lett* **11**:064004. . [Google Scholar](#)
22. ←Taha H (2008) Meso-urban meteorological and photochemical modeling of heat island mitigation. *Atmos Environ* **42**:8795–8809. . [CrossRef](#) [Google Scholar](#)
23. ←Taha H (2015) Meteorological, air-quality, and emission-equivalence impacts of urban heat island control in California. *Sustainable Cities and Soc* **19**:207–221. . [Google Scholar](#)
24. ←Taha H (2009) Urban surface modification as a potential ozone air-quality improvement strategy in California—Phase Two: Fine-resolution meteorological and photochemical modeling of urban heat islands (Altostratus Inc., Martinez, CA), Report CEC-500-2009-071. . [Google Scholar](#)
25. ←Taha H (2008) Urban surface modification as a potential ozone air-quality improvement strategy in California: A mesoscale modelling study. *Boundary Layer Meteorol* **127**:219–239. . [Google Scholar](#)
26. ←Taha H (1997) Modeling the impacts of large-scale albedo changes on ozone air quality in the South Coast Air Basin. *Atmos Environ* **31**:1667–1676. . [CrossRef](#) [Google Scholar](#)

We use cookies on this site to enhance your user experience.
By clicking any link on this page you are giving your consent
for us to set cookies.

[Continue](#)

[Find out more](#)

27. ←Taha H (2005) Urban surface modification as a potential ozone air-quality improvement strategy in California-Phase One: Initial mesoscale modeling (Altostratus Inc., Martinez, CA), Report CEC-500-2005-128. . [Google Scholar](#)
28. ←Edwards PM, et al. (2014) High winter ozone pollution from carbonyl photolysis in an oil and gas basin. Nature **514**:351–354. . [Google Scholar](#)
29. ←Fallmann J, Forkel R, Emeis S (2016) Secondary effects of urban heat island mitigation measures on air quality. Atmos Environ **125**:199–211. . [Google Scholar](#)
30. ←California Energy Commission (2012) Building energy efficiency standards for residential and nonresidential buildings. Title 24 Part 6 and associated administrative regulations in Part 1 (California Energy Commission, Sacramento, CA). . [Google Scholar](#)
31. ←South Coast Air Quality Management District (2016) Final socioeconomic report 2016 air quality management plan (South Coast Air Quality Management District, Diamond Bar, CA). . [Google Scholar](#)
32. ←Building Vectors, ed, Geospatial Repository and Data Management System (GRiD) Cold Regions Research and Engineering Laboratory (CRREL) Engineer Research and Development Center (ERDC) (US Army Corps of Engineers, Washington, DC). . [Google Scholar](#)
33. ←Vahmani P, Ban-Weiss GA (2016) Impact of remotely sensed albedo and vegetation fraction on simulation of urban climate in WRF-urban canopy model: A case study of the urban heat island in Los Angeles. J Geophys Res Atmos **121**:1511–1531. . [Google Scholar](#)
34. ←Finlayson-Pitts BJ, Pitts JN Jr (2000) Chemistry of the Upper and Lower Atmosphere (Academic, San Diego). . [Google Scholar](#)
35. ←Parker DS, McIlvaine JER, Barkaszi SF, Beal DJ, Anello MT (2000) Laboratory testing of the reflectance properties of roofing material (Florida Solar Energy Center, Cocoa, FL). . [Google Scholar](#)
36. ←Prado RTA, Ferreira FL (2005) Measurement of albedo and analysis of its influence the surface temperature of building roof materials. Energy Build **37**:295–300. . [CrossRef](#) [Google Scholar](#)
37. ←Berdahl P, Bretz SE (1997) Preliminary survey of the solar reflectance of cool roofing materials. Energy Build **25**:149–158. . [Google Scholar](#)
38. ←South Coast Air Quality Management District (2016) Final 2016 air quality management plan appendix V: Modeling and attainment demonstrations (South Coast Air Quality Management District, Diamond Bar, CA). . [Google Scholar](#)
39. ←US Environmental Protection Agency (2014) Draft modeling guidance for demonstrating attainment of air quality goals for ozone, PM2.5, and regional haze (US Environmental Protection Agency, Washington, DC). . [Google Scholar](#)
40. ←Ashrafi K, Shafie-Pour M, Kamalan H (2009) Estimating temporal and seasonal variation of ventilation coefficients. Int J Environ Res **3**:637–644. . [Google Scholar](#)

We use cookies on this site to enhance your user experience.
By clicking any link on this page you are giving your consent
for us to set cookies.

Continue

Find out more

41. Xian G, et al. (2011) Change of impervious surface area between 2001 and 2006 in the conterminous United States. *Photogramm Eng Remote Sensing* **77**:758–762. . [Google Scholar](#)

[View Abstract](#)

[Next](#) 

[^ Back to top](#)

 [Article Alerts](#)

 [Email Article](#)

 [Citation Tools](#)

 [Request Permissions](#)

 [Share](#)

[Tweet](#)

[Like 0](#)

 [Mendeley](#)

More Articles of This Classification

Physical Sciences

A nonequilibrium force can stabilize 2D active nematics

Quasicrystalline 30° twisted bilayer graphene as an incommensurate superlattice with strong interlayer coupling

Three-dimensional virtual histology of human cerebellum by X-ray phase-contrast tomography

[Show more](#)

Earth, Atmospheric, and Planetary Sciences

Atmospheric sulfur isotopic anomalies recorded at Mt. Everest across the Anthropocene

Fluctuating radiocarbon offsets observed in the southern Levant and implications for archaeological chronology debates

Related Content

Cited by...

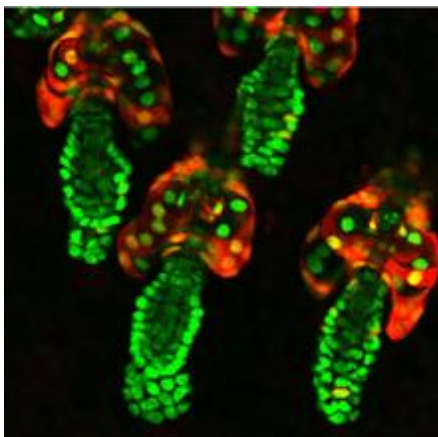
We use cookies on this site to enhance your user experience. By clicking any link on this page you are giving your consent for us to set cookies.

[Continue](#)

[Find out more](#)

▶ **Similar Articles**

YOU MAY ALSO BE INTERESTED IN



Inner Workings: Microscopy lights up stem cells in action

In the midst of a microscopy boom, stem cell researchers are coming up with inventive techniques for capturing live images of these enigmatic cells in their native habitats.

Image courtesy of Panteleimon Rempelas (University of Pennsylvania, Philadelphia).



News Feature: Life after the asteroid apocalypse

Sixty-six million years ago, an asteroid wiped out a huge swath of life on planet Earth. But could this and similar impacts have helped kick-start life itself?

Image courtesy of Detlev van Ravenswaay/ScienceSource.



RNA origin in warm little ponds

Ralph Pudritz and Ben Pearce describe a model of how RNA-based life could have originated on the early Earth.

Listen



[Past Podcasts](#) | [Subscribe](#)

PNAS QnAs

PNAS QnAs with Joanne Chory, winner of the Breakthrough Prize in life sciences.

We use cookies on this site to enhance your user experience. By clicking any link on this page you are giving your consent for us to set cookies.

[Continue](#)

[Find out more](#)



Climate change and dengue in Latin America

Limiting global mean temperatures to 2°C above pre-industrial levels could prevent approximately 2.8 million dengue cases in Latin America per year by the end of the century, compared with a business-as-usual scenario, according to a study.

Image courtesy of Pixabay/Alexas_Fotos.

We use cookies on this site to enhance your user experience. By clicking any link on this page you are giving your consent for us to set cookies.

[Continue](#)

[Find out more](#)

Cooperation and reward in mongooses



Jupiter-Venus eccentricity cycles
Accuracy in face identification
Phylogeny of ray-finned fishes
Protection and mediation of cytomegalovirus

Current Issue

Submit

Sign up for Article Alerts

Enter Email Address

Sign up



We use cookies on this site to enhance your user experience. By clicking any link on this page you are giving your consent for us to set cookies.

Submit Manuscript

Continue

Find out more

 [Twitter](#)

 [Facebook](#)

 [RSS Feeds](#)

 [Email Alerts](#)

Articles

[Current Issue](#)

[Latest Articles](#)

[Archive](#)

PNAS Portals

[Classics](#)

[Front Matter](#)

[Teaching Resources](#)

[Anthropology](#)

[Chemistry](#)

[Physics](#)

[Sustainability Science](#)

Information for

[Authors](#)

[Reviewers](#)

[Press](#)



[Feedback](#) [Privacy/Legal](#)

Copyright © 2018 National Academy of Sciences.

We use cookies on this site to enhance your user experience. By clicking any link on this page you are giving your consent for us to set cookies.

[Continue](#)

[Find out more](#)